Polymer 267 (2023) 125626

Contents lists available at ScienceDirect

Polymer

journal homepage: www.elsevier.com/locate/polymer

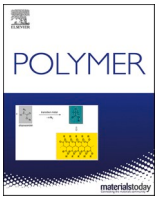

Solvent induced effect on morphology and properties of disulfonated polyarylene ether sulfone block copolymer membranes for PEMFC applications

Natalie Y. Arnett [a,c,*], Sanjay Kumar Devendhar Singh [a,c,**], D'Andra Moxey [a], Samaiyah K.A. Mason [a], Rebekah Sweat [b,c], Emily Plunket [d], Robert Moore [d]

[a] Department of Chemistry, Florida A&M University & Florida State University, Tallahassee, FL, USA
[b] High-Performance Materials Institute (HPMI), Tallahassee, FL, USA
[c] FAMU-FSU College of Engineering, Tallahassee, FL, 32310, USA
[d] Department of Chemistry and Macromolecules Innovation Institute, Virginia Tech, Blacksburg, VA, USA

ARTICLE INFO

Keywords:
Dynamic mechanical analyzer (DMA)
Flory-Huggins interaction parameters ($\chi_{P\text{-}S}$)
Poly (arylene ether sulfone) (PAES)
Polymer membranes
Solvent effect

ABSTRACT

A systematic investigation to ascertain a fundamental understanding of the residual solvent effect on the bonding characteristics, thermal and mechanical properties of poly(arylene ether sulfone) (PAES) membranes was carried out. Transparent PAES membranes were synthesized using different solvents, which include dimethylformamide (DMF), dimethylacetamide (DMAc), dimethylsulfoxide (DMSO), and *N*-methyl-2pyrrolidone (NMP). A correlation was established between polymer-solvent interaction using Hansen solubility parameters (HSP) and Flory-Huggins interaction parameters ($\chi_{P\text{-}S}$). Proton conductivity, thermogravimetric analysis (TGA), dynamic mechanical analysis (DMA), and FTIR were correlated with $\chi_{P\text{-}S}$ parameter. PAES membrane derived using DMF solvent exhibited the highest proton conductivity (0.133 ± 0.01 S•cm^{-1}). Scanning electron microscopy (SEM) confirmed the formation of defect-free membranes. The presence of residual solvent in the membranes resulted in a plasticizer effect which was confirmed through storage modulus behavior from DMA. This study will act as a standard protocol for the development of high-performance PAES membranes with desired properties for polymer fuel cells applications.

1. Introduction

Poly (arylene ether)s are widely known engineering thermoplastics with a wide variety of desirable properties such as high thermal, hydrolytic, and oxidative stability, good mechanical strength, and high glass transition temperatures [1]. Initial interests in poly (arylene ether) s homopolymers and copolymers began with the synthesis of polysulfone condensation polymers from p, p'- dihalodiphenyl sulfones and *p*-phenylenedithiols by Kreuchunas [2]. The attraction to Poly (arylene ether)s stems from its versatility in using a diverse array of aromatic biphenol and dihalide monomers resulting in a wide range of amorphous or semicrystalline commercially available high-performance polymers for resins and membrane applications [3,4]. Sulfonated poly (arylene ether)s are being investigated as an alternative to commercially available perfluorinated proton exchange membranes (PEM) such as Dupont Nafion® [4–6]. The latter exhibited some drawbacks, such as a reduction in proton conductivity at high temperatures (greater than 80 °C), high cost, and high methanol crossover [6]. On the other hand, membranes derived from poly(arylene ether sulfone) (PAES) were found to possess good stability towards acids and oxidation, high glass transition temperature (T_g), hydrolytic stability, and excellent mechanical integrity [7]. Despite advancement and novel methods to synthesize PAES membranes, the transport properties and selectivity depend mainly on the fabricating methodology and materials used, which ultimately affects membrane performance [6,8]. Therefore, the physical properties of PAES membranes, including crystallinity, fractional free volume, porosity, mechanical properties, and sorption sites, can be fine-tuned by choosing an appropriate fabrication method [9,10].

Most of these properties are directly or indirectly correlated to solvent-polymer interaction, with casting solvent playing an essential

* Corresponding author. Department of Chemistry, Florida A&M University & Florida State University, Tallahassee, FL, USA.
** Corresponding author. Department of Chemistry, Florida A&M University & Florida State University, Tallahassee, FL, USA.
E-mail addresses: narnett@eng.famu.fsu.edu (N.Y. Arnett), sd22bd@fsu.edu (S.K. Devendhar Singh).

https://doi.org/10.1016/j.polymer.2022.125626
Received 17 October 2022; Received in revised form 16 December 2022; Accepted 20 December 2022
Available online 21 December 2022
0032-3861/

role in defining the membrane properties [9,11]. Investigations on solvents having closer soluble parameters to that of polymers revealed that the polymers had a better environment for polymer chain unfolding and achieved a thermodynamically stable low entropy configuration [11,12]. Additionally, membranes cast using solvents having closer solubility parameters to that of polymers exhibited smoother surface morphology [13]. It was also observed that the membranes fabricated using solvents having higher molar volume (V_m) led to larger fractional free volumes due to its slow evaporation and also it is present as residuals in the membrane [13]. Robertson et al. [14] using ^{1}H NMR spectroscopy found that the hydrogen bonding interaction between sulfonic acid group of poly(ether ether ketone) and residual dimethylformamide are stronger compared to that of dimethylacetamide solvents which led to decrease in their proton conductivity. Similarly, residual solvents could induce heterogeneity or formation of semi-crystalline phases in the polymer membranes which will have drastic effect on the final properties [15]. Studies have shown that presence of crystalline/semicrystalline phases decreases diffusivity, permeability, and mechanical durability of the fabricated membranes [16,17]. Therefore, PEM technologist often prefers membranes having a very low crystalline phase or amorphous polymeric membranes [17]. However, the formation of semi-crystallline phases in the membranes is inevitable; thus, low molecular plasticizers are utilized to make flexible membranes and glassy polymers [15,18]. Studies have also shown that the complete removal of residual solvent from the membranes below the T_g is difficult [12]. Residual solvent can also act as a plasticizer which could help to improve the membrane flexibility (plasticization) during fabrication [16,19]. Studies to explore the effect of complete removal of solvents from the membrane have been investigated [16]. However, thermal treatment below T_g results in dense membranes while heating the polymer above T_g, stiffens the polymer chain and inhibits the segmental motion [12,16]. Consequently, polymer chain collapses due to solvent-induced microstructure (antiplasticizer) [12]. Therefore, it is important to understand the effect of solvent-induced microstructure and the influence of residual solvents on the thermal and mechanical properties of PEM membranes.

In general, the type of casting solvent can be correlated to various membrane properties like proton conductivity [20], gas transport [21], permeability [22], and morphology [23]. Some of the most commonly used casting solvents in membrane technology are dimethylformamide (DMF, b.p.: 153 °C), dimethylacetamide (DMAc, b.p.: 165 °C), Dimethyl sulfoxide (DMSO, b.p.: 189 °C), and *N*-methyl-2pyrrolidone (NMP, b.p.: 202 °C). Research has demonstrated that the interaction between the polymers and these solvents is different, resulting in varied solvent-induced microstructures [15,20]. ^{1}H NMR spectroscopy studies on sulfonated polymers and Torlon membranes revealed that the residual solvent interacts strongly to form hydrogen bonds which in turn improved the CO_2/CH_4 diffusivity in the former while the latter showed decreased conductivity [12,14,20]. DMF was shown to readily form hydrogen bonding (H-bonding) complexes between its amide functional group and sulfonic acid at low temperatures (60 °C), while DMAc was less susceptible to engage in hydrogen-bonding, which only occurred above 100 °C [14]. Investigation of sulfonated poly(ether ether ketone) (sPEEK) membranes demonstrated that DMF and/or DMAc often resulted in membranes with low crystallinity [24]. On the other hand, sPEEK membranes cast using DMSO resulted in a more crystalline structure, decreasing their proton conduction [24]. Further studies carried out on sPEEK film prepared in DMAc, DMF, and DMSO for vanadium redox flow battery (VRFB) showed similar results where stronger polymer-solvent interactions between sPEEK and DMSO were achieved because, in this case, three DMSO molecules interacted with one $–SO_3H$ group to form strong H-bonding compared to one DMF molecule per $–SO_3H$ [25]. The weaker DMF-sPEEK interactions allowed higher VRFB single-cell performance and discharge capacity retention [25].

PAES membranes exhibited exceptional thermal, mechanical, and chemical properties. The interaction between the sulfonic acid group of the polymer with residual solvent can result in plasticization resistance due to the formation of hydrogen bonding. Investigations on the effect of casting solvent on sulfonated PAES membranes are limited. The present study will help to establish a correlation between physical morphology, mechanical integrity, and residual solvent. In this study, disulfonated poly(arylene ether sulfone) membranes were fabricated in-house using four solvents: DMAc, NMP, DMSO, and DMF. Hensen solubility parameter (HSP) and Flory-Huggins interaction parameters were elucidated to understand the polymer-solvent interactions. The derived PAES membranes were investigated and characterized prior to conversion of the sulfonate potassium salt to the sulfonic acid form using attenuated total reflection Fourier transform infrared spectroscopy (ATR-FTIR), thermogravimetric analysis (TGA), scanning electron microscopy (SEM), and dynamic mechanical analysis (DMA). This study will help to establish a correlation between polymer-solvent interactions on the final properties of PAES membranes with desired properties for polymer fuel cells applications.

2. Experimental

2.1. Materials and sulfonated poly(arylene ether sulfone) membrane preparation

4.4′- Disulfonated biphenol-based poly(arylene ether sulfone) random copolymer was purchased from Akron Polymer Systems. NMP was purchased from Oakwood Chemical, N. Estill, SC, USA, while DMAc, (≥99.8%), DMF (≥99.8%), and DMSO (≥99.9%) were purchased from Sigma Aldrich, St. Louis, MO, USA. In this study, all solvents were used as recieved. Fabrication of PAES membranes is described in detail elsewhere [26,27]. In a typical method, an appropriate quantity of polymers (5% w/w) was dissolved in a solvent and filtered through a 0.45 μm PTFE syringe filter. Simultaneously, polymers solution casting and solvent evaporation were performed on a dry clean glass plate in the presence of a heating lamp. After 24 h, the fabricated membranes were removed from the glass plates and kept in a vacuum oven at 50 °C. The reason for choosing 50 °C in vacuum condition was to minimize the free volume changes (packing density decrease) which could impact both permeability, mechanical and proton conductivity in PAES membrane. Also, evaporation of residual solvent in vacuum condition at high temperatures could induce defect formation due to the pressure build-up. Hence, in this study, drying of all PAES-solvent membranes were carried out at 50 °C in vacuum. The membranes derived were transparent and defect free (like cracks or porosity). The membranes derived from respective solvents like DMSO, DMF, NMP, and DMAc were denoted as PAES-DMSO, PAES-DMF, PAES-NMP, and PAES-DMAc, respectively.

2.2. Membrane characterization

2.2.1. Fourier transform infrared spectroscopy (ATR-FTIR)

The FTIR spectra of all PAES membranes were carried out using an Agilent Technologies FTIR Cary 630 instrument. The Agilent's program software of MicroLab PC was used to record the spectrum in the range of 4000 to 500 cm^{-1} at an average of 200 scans to analyze the functional groups present in the PAES membranes.

The procedure to determine the magnitude of hydrogen bonding using FTIR has been previously reported wherein the O–H stretching frequencies of PAES membranes fabricated by using different solvents were compared with the O–H stretching frequency of pristine PAES polymers [26]. Deviation in wavenumber of polymer from the wavenumber of the baseline polymer can be attributed to changes in H-bonding due to the solvent. The magnitude of hydrogen bonding was estimated using Eq. (1):

$$\text{The magnitude of H}-\text{bonding} = \tilde{\upsilon}_{no\ solvent} - \tilde{\upsilon}_m \quad (1)$$

where $\tilde{\upsilon}_{\text{no solvent}}$ and $\tilde{\upsilon}_m$ indicate the wavenumber of control membrane

(no solvent) and PAES-solvent membrane (solvent: DMSO, DMF, NMP, and DMAc), respectively.

2.2.2. Thermogravimetric Analysis (TGA)

TGA analysis was employed to investigate the thermal stability and to detect the small fraction of residual solvent present in PAES membranes using a TA Instruments TGA Q50. All PAES-solvent membranes were heated from room temperature to 500 °C at a heating rate of 10 °C•min^{-1} in an N_2 atmosphere. The temperature at 5% weight loss was used as the degradation temperature (T_d).

2.2.3. Differential Scanning Calorimetry (DSC)

The glass transition temperatures (T_g) of the PAES-solvent membranes were determined using TA Instrument DSC Q2500. In a typical analysis, about 10 mg of dried PAES-solvent membranes were equilibrated at 100 °C for 30 min. Subsequently, the samples were cooled to room temperature and reheated from room temperature to 400 °C at 10 °C•min^{-1}. All DSC analyses were performed under an N_2 atmosphere, and the T_g of the respective membranes was determined from the midpoints of the changes in the slopes of the DSC curve of the second heating cycle. DSC thermograms were recorded from room temperature to 400 °C at a rate of 10 °C•min^{-1}.

2.2.4. Dynamic Mechanical Analysis (DMA)

It is well known that most of the polymeric membrane do not follow a linear stress-strain relationship and do not obey Hooke's law ($\sigma = E\varepsilon$), where E is Young's modulus. This polymeric membrane exhibits viscoelastic behavior. Therefore, their corresponding stress and strain are not in-phase, and hence their modulus (E*) becomes a complex function:

$$|E^*| = E' + iE'' = \sqrt{(E')^2 + (E'')^2} \tag{2}$$

Where E' and E" are in-phase (storage modulus) and out-of-phase (loss modulus) components of complex modulus, E*. The loss angle (δ) or amount of energy dissipated as heat can be computed using:

$$tan\ \delta = \frac{E''}{E'} \tag{3}$$

Therefore, to understand the mechanical behavior and also to elucidate the T_g of the PAES-solvent membranes. DMA experiment were carried out using ARES-G2, TA Instruments, Delaware, USA in the orthogonal superposition in clamped tension. Temperature sweeps were completed from 30 °C to 425 °C at a rate of 10 °C•min^{-1}. A 0.1% strain oscillation was measured at 1 Hz frequency with 1 N initial static force with an oscillation amplitude of 10 μm.

2.2.5. Solubility parameter

It is well established that the properties and the morphology of the polymer membrane depends strongly on the casting solvent and the relative interaction strength between the polymer and solvent used [13,28,29]. In general, the interaction between polymer and solvent system are divided into three types: polymer-polymer, polymer-solvent, and solvent-solvent [13,28,29]. Therefore, it is a prerequisite to identify a suitable solvent for making membranes with desirable properties. A good solvent often unwinds the polymer to a maximum extent to favor maximum polymer-solvent interaction (low entropy configuration) [12,29]. The extent of affinity between polymer and solvent can be estimated using the Hansen solubility parameter (HSP) [12,13,29]. Hansen proposed a practical way to measure the total cohesion parameter (δ_t) using the Hildebrand parameter wherein the dispersion (δ_d), polar (δ_p), and hydrogen bonding parameters (δ_H) are taken into consideration. Eqn. (4) can be used to determine (δ_t) [13,29,30].

$$\delta_t = \sqrt{\delta_d + \delta_p + \delta_h} \tag{4}$$

Hoftyzer–Van Krevelen method demonstrated that the HSP parameters could be estimated using the group contribution method for both polymers and solvent [29]. The dispersion (δ_d), polar (δ_p), and hydrogen bonding forces (δ_H) for solvent and PAES polymer can be computed using Eqs. (5)–(7).

$$\delta_d = \frac{\sum F_{di}}{V} \tag{5}$$

$$\delta_p = \frac{\sqrt{\sum F_{pi}^2}}{V} \tag{6}$$

$$\delta_h = \sqrt{\frac{\sum E_{hi}}{V}} \tag{7}$$

where F_{di}, E_{hi}, and V are molar attraction constant, cohesive energy, and molar volume, respectively. The dissolution process between PAES polymer-solvent pair was estimated using Flory-Huggins interaction parameters ($\chi_{P\text{-}S}$) [29]:

$$\chi_{P-S} = 0.34 + \frac{V_m}{RT}(\delta_P - \delta_S)^2 \tag{8}$$

where V_m, R, T, δ_s, and δ_p are the molar volume of solvent, the universal gas constant, temperature, and total solubility parameter of solvent and PAES polymer, respectively.

2.2.6. Scanning Electron Microscopy (SEM) and proton conductivity

Microstructural and morphological analysis of the PAES membranes derived in this study were carried out using Phenom XL G2 scanning electron microscopy (SEM) supplied by DOW®. The membranes were cut into definite shape. To avert the surface charging effect, all PAES membranes were coated with gold to a thickness 7 nm using Cressington Sputter Coater 108. The proton conductivity of the acidified PAES membranes was carried out using a SolarTron SI 1287 potentiostat. In a typical experiment, PAES membranes were equilibrated in deionized water for 24 h, followed by rinsed in deionized water. The clamped membranes were subsequently submerged in water and ran for three sequential cyclic voltammetry (CV) in open circuit potential mode (scan rate: 10 mV s^{-1}) between −0.25 and 0.25. The resistance (R) from CV was used to determine the proton conductivity of the membrane using Eq. (9) where the distance between the electrode (L) is 0.425 cm (L) while T and W were thickness and width of the PAES membrane used.

$$\sigma = \frac{L}{T \times W \times R} \tag{9}$$

3. Results and discussion

3.1. HSP and Flory-Huggins interaction parameters ($\chi_{P\text{-}S}$)

In this study, to understand the interaction of polymer and solvent, HSP and Flory-Huggins interaction parameters ($\chi_{P\text{-}S}$) of polymer-solvent pairs were estimated using the methodology as described in detail elsewhere [13,29]. HSP of PAES polymer, DMF, DMAc, DMSO, and NMP were estimated from the group contribution method, while Hoftyzer–Van Krevelen method was used to compute the $\chi_{P\text{-}S}$ values (Table 1) [13,29]. A more negligible difference in the total cohesion solubility parameter (δ_t) between the solvent and polymer implies better interaction [12,29]. In other words, a closer δ_t value of the polymer to that of solvent implies that the polymers undergoes chain unfolding to a larger extent which in turn enhances the dissolution of the polymer in the solvent [12,31,32]. In this study, it was found that the difference in the cohesion solubility parameter between PAES-solvent system $|\delta_{S\text{-}P}|$ was found to be 0.36 (PAES-DMF), 1.44 (PAES-DMSO), 2.3 (PAES-NMP) and 2.49 (PAES-DMAc). Similarly, Flory-Huggins parameters were estimated to understand the miscibility levels of the PAES polymer and solvent [29]. Table 1 shows that the computed Flory-Huggins value for PAES-DMF system to be lowest while PAES-DMAc system exhibited the

Table 1
Hansen solubility parameters and Flory-Huggins interaction parameters using Hoftyzer–Van Krevelen method.

S. No.	Materials	Solubility parameter $\left(MPa^{1/2}\right)$				$\chi_{P\text{-}S}$
		Dispersion parameter (δ_d)	Polar parameter (δ_p)	Hydrogen-bonding parameter (δ_H)	Total cohesion parameter (δ_t)	
1.	*N,N*-Dimethylformamide (DMF)	17.4	13.7	11.3	24.90	0.34
2.	*N,N*-Dimethylacetamide (DMAc)	16.8	11.5	10.2	22.77	0.57
3.	Dimethyl sulfoxide (DMSO)	18.4	16.4	10.2	26.70	0.40
4.	1-Methylpyrrolidin-2-one (NMP)	18.0	12.3	7.2	22.96	0.55
5.	Disulfonated poly(arylene ether sulfone) copolymers	21.97	8.35	9.3	25.26	–

highest values. Therefore, it could be concluded that DMF has better miscibility with PAES polymer compared to that of DMAc solvents. Similar trend was observed when $\chi_{P\text{-}S}$ values of Torlon-400 T polymer membranes was calculated using different solvents (DMF, DMAc and NMP) [12]. It was observed that $\chi_{P\text{-}S}$ values for Torlon-400 T polymers with DMF was lowest compared to that of DMAc and NMP solvents [12]. Therefore, in this study, it could be concluded that the estimated HSP and Flory-Huggins interaction parameters lead to similar conclusion i.e., the misibility of PAES in DMF solvents are relatively better compared to that of other solvents (DMAc, NMP and DMSO). In otherwords, DMAc solvents could result in differential densification of PAES membranes, therefore, care should be taken in choosing the appropriate solvents during membrane fabrication. Studies have shown that differential topological properties has some advantage in gas permeation technologies, for instance, Torlon-400 T fabricated using DMAc solvents has better selectivity (or separation) of CO_2/CH_4 gases [12]. Therefore, depending upon the applications, the properties of the membrane can be tuned-in by choosing appropriate solvents. Care should be taken on using HSP and $\chi_{P\text{-}S}$ parameters in highly crystalline ionomers/polymers wherein heat of fusion plays a major role during dissolution and it has to be considered in the calculation of free enthalpy. Furthermore, HSP and $\chi_{P\text{-}S}$ parameters assumes that the cohesive energy is divided into only three parts namely atomic dispersion, molecular dipolar interaction and hydrogen-bonding and all other interaction (like hydrophilicity) are not considered in these calculations.

3.2. ATR-FTIR

ATR-FTIR analysis was utilized to confirm the functional groups present in PAES membranes synthesized using different solvents. Fig. 1

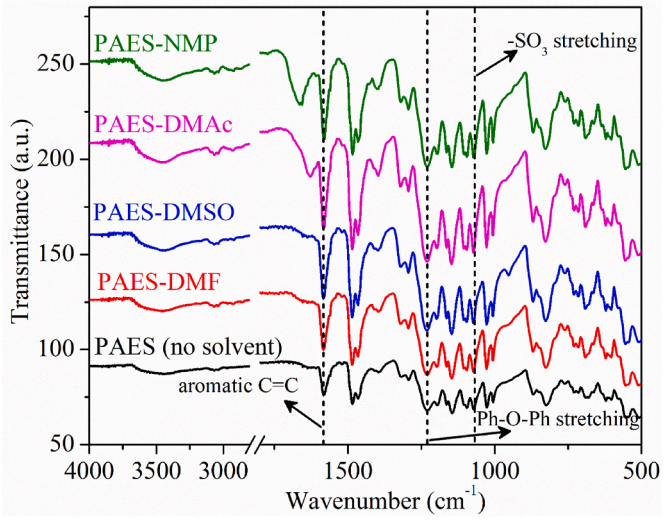

Fig. 1. FTIR spectrum of PAES membrane where (a) PAES with no solvent, (b) PAES-DMF, (c) PAES-DMSO, (d) PAES-DMAc, and (e) PAES-NMP.

shows the FTIR spectrum of PAES polymer, PAES-DMSO, PAES-DMF, PAES-NMP, and PAES-DMAc membranes. A broad peak around 3500 cm^{-1} corresponds to –OH stretching, while a strong peak at 1232 cm^{-1} confirms the presence of aromatic ether linkage. Similarly, peaks observed at 1029 and 1095 cm^{-1} confirm the presence of symmetric and asymmetric stretching of the sulfonic acid group (-SO_3) [33,34]. It was observed that the relative peak intensity corresponding to PAES-NMP and PAES-DMAc membranes for –SO_3 groups were more intense compared to that of PAES-DMSO and PAES-DMF membranes (Fig. 1). This could probably be due to the presence of flexible PAES structures as a result of weaker solvent (NMP/DMAc)-PAES interaction. Furthermore, PAES-NMP and PAES-DMAc membranes showed an additional peak at 1666 and 1628 cm^{-1}, respectively, which could be attributed to –C═O stretching of the amide group coupled with the interaction between residual solvents and –SO_3H functional groups (Fig. 1). Previous studies reported that the presence of residual solvent is likely due to the high boiling of the solvent which might remain trapped during membrane casting [35]. In PAES membrane, residual NMP and DMAc solvents resulted in the appearance of additional peaks at 1666 and 1628 cm^{-1}, respectively [14,20,36]. DMAc ability to undergo conjugative group shifts to from aldehyde to alcohol or vice versa structures allows for extra conformational stability compared to NMP [14]. Hence, the peak shifts to a lower wavelength.

3.3. The determination of magnitude of hydrogen bonding

Studies carried out on sulfonated PAES-2,4,6-triphoshphonic acid-1,3,5-triazine (TPAT) membrane had shown that the magnitude of H-bonding could be estimated using FTIR [9]. It was also shown that the infrared spectral features are significantly different for membranes derived from different solvents, and their relative H-bonding intensities depend on the type of solvent used [37]. It was observed that the shifts of the order of magnitude in the wavenumbers and considerable increases in the IR bands intensity are associated with interacting functional groups with solvent to form H-bonding bridges [38]. The deviation in the –OH peak wavenumber of the polymer membranes below the –OH stretching frequency of PAES with no solvent can be attributed to H-bonding interactions between polymer and solvent [39]. In general, increased H-bonding would restrict the mobility of the –OH group (stretching), resulting in peak shift to lower wavenumbers. Fig. 2 illustrates the H-bonding magnitude numbers for wavenumber and intensity changes compared to PAES with no solvent and membranes prepared in different solvents. In this study, an amide II structure (DMF, NMP and DMAc) appearing around 1582 cm^{-1} was investigated to understand the role of residual solvent on the H-bonding structures with the PAES membrane [40]. The baseline of all PAES membranes prepared with different solvents and PAES with no solvent was corrected using linear intercept method in the range of 1535–1603 cm^{-1}. Fig. 2 shows the interaction region due to amide II form (residual solvent: NMP, DMAc and DMF) and DMSO with the C═C bond of benzene ring of PAES membrane. Fig. 2 confirms that the peak intensity increases with $\chi_{P\text{-}S}$ parameter. It should be noted that the C═C bond of the benzene ring from the PAES membrane also appears around 1586 cm^{-1} and the

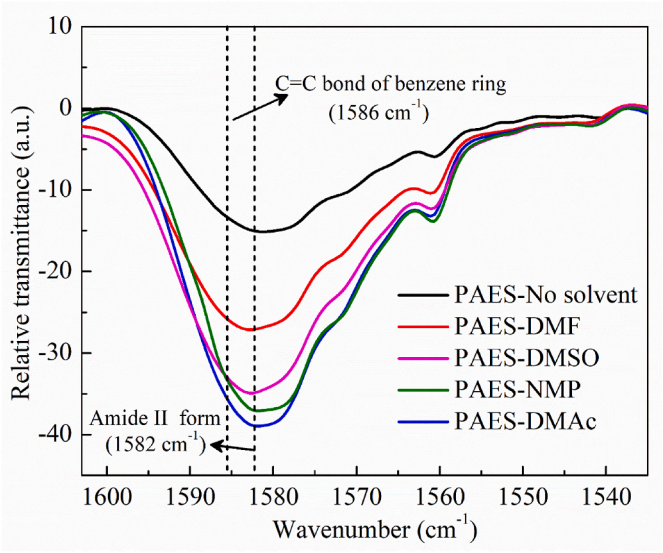

Fig. 2. Normalized FTIR spectrum of PAES membrane comprising of PAES with no solvent, PAES-DMF, PAES-DMSO, PAES-DMAc, and PAES-NMP.

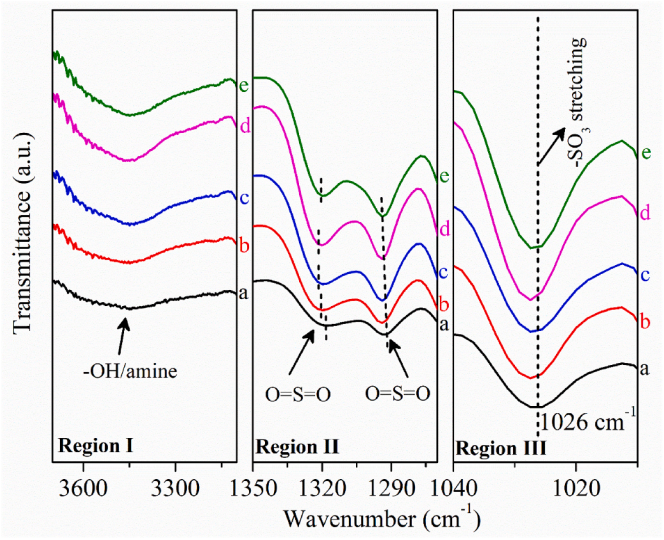

Fig. 3. Selected region of FTIR spectrum of PAES membrane where (a) PAES with no solvent, (b) PAES-DMF, (c) PAES-DMSO, (d) PAES-DMAc, and (e) PAES-NMP.

interaction with the DMSO also appears at the same region [25]. It is well known that maximum 3 molecules of DMSO can undergo H-bonding and dipole-dipole interactions with the PAES polymer (sulphonic acid group). Therefore, the observed peak is due to the resultant effect. Fig. 2 shows that the relative peak intensity decreases and followed the order PAES-DMAc > PAES-NMP > PAES-DMSO > PAES-DMF > $PAES_{(no\ solvent)}$. A closer look at the trend reveal that the peak intensity were correlated to Flory-Huggins interaction parameters ($\chi_{P\text{-}S}$). In other words, solvent which had the lowest difference in total cohesion parameter (δ_t) compared to that of the polymer exhibited the lowest relative peak intensity. It further confirms that the concentration of residual solvent trapped in the PAES membrane increases with $\chi_{P\text{-}S}$.

Wavelength shifts represent the effect of hydrogen bonding on the symmetric stretch of the hydroxyl peak caused by the deviation of the wavenumbers from PAES-NS (3450 cm^{-1}) (NS indicates no solvent). Peak intensity changes were determined by differences in PAES-NS intensity to solvent cast membranes. To understand the effect of solvent on peak shift, three different FTIR regimes were selected: Region I- 3100 to 3700 cm^{-1} (-OH and/or $–NH_2$ stretching), Region II- 1270 to 1350 cm^{-1} (Ph-*O*-Ph stretching and amide III structure), and Region III- 1010 to 1040 cm^{-1} (O═S═O stretching). These three peak regions were selected because the sulfonate, amide and hydroxyl functional groups can form an H-bonding (Fig. 3). It was observed that all samples, including PAES with no solvent, exhibited the peak maxima around 3439 cm^{-1}, indicating that the H-bonding did not impact any shift in the wavelength. However, PAES-DMAc membranes exhibited a shallow peak compared to other PAES-polymer membranes. This could be due to the presence of a slightly higher quantity of residual solvent in the PAES membrane and forming stronger H-bonds. Similarly, using a different solvent, the O═S═O stretching also substantially affected the PAES membrane formation. Fig. 3 shows that both PAES-NMP (1320.98 cm^{-1}) and PAES-DMAc (1321.52 cm^{-1}) exhibited peak shifts, resulting in shallow peak intensity. On the other hand, PAES-DMF (1319.91 cm^{-1}) and PAES-DMSO (1320.43 cm^{-1}) exhibited a slight peak shift when compared to the PAES-NS membrane (1318.42 cm^{-1}). In comparison to the –OH region (3700–3100 cm^{-1}), more considerable peak intensities variations were observed in the $–SO_3$ peaks between 1040 and 1010 cm^{-1}, indicating more interactions between sulfonic acid groups and solvent (Fig. 3). The trend in peak intensity differences is comparable to shift changes where: PAES-DMF (1026.95 cm^{-1}) <PAES-DMSO (1027.16 cm^{-1}) < PAES-NMP (1027.34 cm^{-1}) < PAES-DMAc (1027.66 cm^{-1}). These observations are in-line with HSP and Flory-Huggins interaction parameters which exhibited that the DMAc has the highest values, which might have led to forming of a solvent cluster in PAES membrane via H-bonding. On the other hand, DMF and DMSO had a low solubility interaction parameter (HSP and Flory-Huggins interaction parameters ($\chi_{P\text{-}S}$)). Therefore, it was easy to remove these solvents to a maximum extent during fabrication. The changes for PAES membranes differ from published research that demonstrated that DMF is particularly prone to hydrogen bonding with $–SO_3H$ groups in sPEEK, while no evidence of hydrogen bonded to DMAc could be observed [41]. Therefore, the changes observed may be related to residual solvents remaining in the membrane.

3.4. *The effect of solvents on thermal properties and microstructure*

Fig. 4 shows the thermal decomposition (T_d) of the pristine PAES and PAES membranes fabricated using different solvents from room temperature to 500 °C in inert atmosphere. All solvent-based PAES membranes exhibited two distinct weight-loss while PAES-NS exhibited only

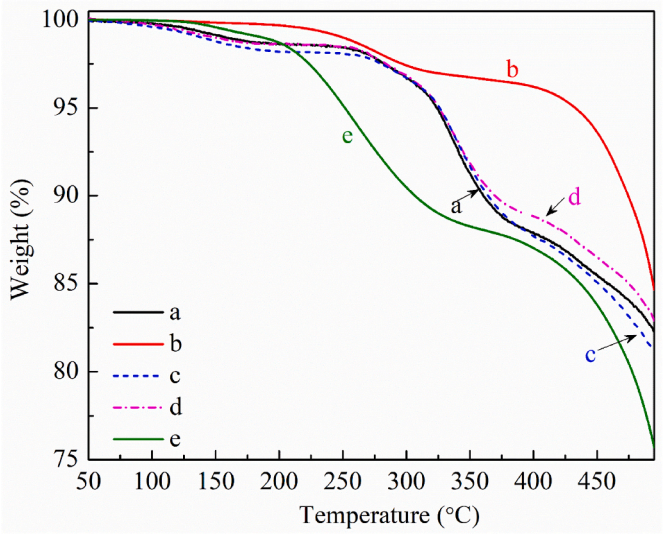

Fig. 4. Thermal Analysis of (a) PAES with no solvent, (b) PAES-DMF, (c) PAES-DMSO, (d) PAES-DMAc, and (e) PAES-NMP.

a single loss event. PAES membranes revealed an initial weight loss between 100 and 300 °C) attributed to sulfonic group decomposition, while the loss at ~450 °C is related to the degradation of the PAES backbone [20].

Fig. 4 confirms that PAES membranes fabricated using different solvents had different microstructure and membrane properties; hence, different thermal behaviors were exhibited. For instance, PAES-NMP membrane exhibited low thermal stability compared to PAES-DMF membrane (stable up to 434 °C). From the plot (Fig. 4), it is clear that HSP and Flory-Huggins interaction parameters ($\chi_{P\text{-}S}$) correlate well for the PAES-DMF membrane. The thermal stability of the PAES-NMP membrane could be due to two plausible reasons: a) $\chi_{P\text{-}S}$ interaction parameter is not favorable, therefore resulting in partial polymer chain unfolding and b) high boiling (202 °C) and larger molar volume of NMP solvent, could require additional processing time to remove excess residual solvent during membrane fabrication [17]. The thermal behavior of PAES-DMSO and PAES-DMAc membranes almost follow a similar trend up to 350 °C. Above 350 °C, PAES-DMSO decomposes first, followed by PAES-DMAc membranes. Therefore, the thermal stability of PAES membranes fabricated in this study followed the following trend: PAES-NMP < PAES-DMSO < PAES-DMAc < PAES-DMF. The trend connecting T_d to boiling point temperature is related to the amount of solvent remaining in the films after fabrication has been reported previously [26]. All the membranes displayed temperatures lower than the pristine PAES-NS polymer. This was expected as research has shown that the presence of residual solvents plasticizes the membrane [17].

Fig. 5 shows the differential scanning calorimetry analysis of PAES membranes and PAES-NS samples. It is well documented that the residual solvent is typically released around the T_g due to polymer plasticization and molecular motion [17]. DSC analysis (Fig. 5) of the membranes shows the presence of multiple transitions for the PAES membranes prepared with DMSO, DMAc, and DMF solvents. In general, all PAES membranes prepared in this study exhibit both amorphous and semi-crystalline properties with excess free volume which will retain residual solvent at the molecular level during PAES membrane fabrication step. Therefore, the interaction of the polymer with the residual solvent and the concentration of residual solvent present in the membranes both affect crystallization and the T_g. The first transition was related to solvent loss from the membrane, while the second transition corresponds to the onset of the alpha transition of the PAES membrane. The endothermic peak observed immediately after the T_g could be due to the molecular relaxation which usually appears as a result of transition from rigid to flexible structures on heating. PAES-NMP membrane displayed a crystallization transition (T_c) around 180 °C, which is uncommon for amorphous PAES. The presence of T_c could be attributed to solvent-induced semicrystallization, which has been demonstrated in high-performance polymers with high glass transition temperatures [42]. DSC analysis of PAES-DMAc did not show any substantional changes and their corresponding curves are shown in Fig. S1 (supplementary). Fig. 6 shows the representative SEM image of the PAES membrane fabricated using DMSO solvent. SEM images all other samples (PAES-DMF, PAES-NMP and PAES-DMAc) are shown in Fig. S2 (supplementary). In general, SEM images of all samples revealed that the fabricated membranes are crack free, smooth, and uniform in microstructure (no phase segregation). No difference in membrane density was observed using dimensional measurement. Cross-sectional examination of PAES revealed that the fabricated membranes exhibited the thickness of about 30 ± 2 μm.

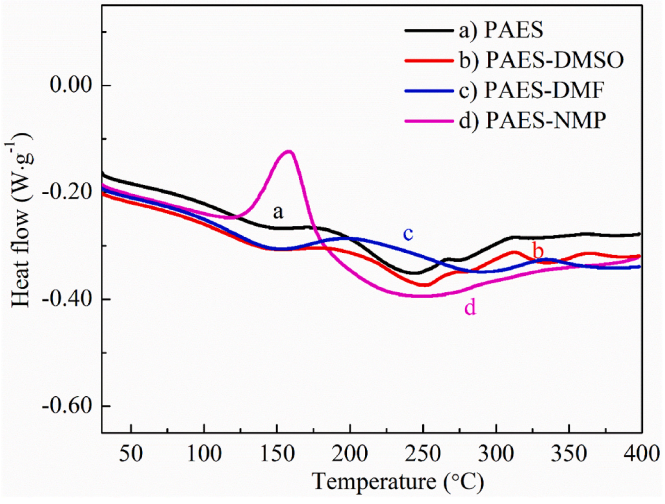

Fig. 5. DSC analysis of (a) PAES with no solvent, (b) PAES-DMSO, (c) PAES-DMF, and (d) PAES-NMP.

3.5. Dynamic mechanical analyzer (DMA) and proton conductivity

Fig. 7 shows the DMA curve of PAES-DMF, PAES-DMSO, PAES-NMP, and PAES-DMAc polymer membrane. The storage modulus (E') and the damping (tan δ) spectra with temperature helps to estimate the glass transition temperature (T_g). The decrease in storage modulus and the peak of tan δ were used to estimate the T_g values. Generally, it was observed that the storage modulus and tan δ of all the PAES membranes (≈2000 MPa @RT) synthesized in this study were higher than that of commercial Nafion® (≈300–600 MPa @RT) [31,43]. In general, it is well known that the presence of sulfonated ionic groups in the polymer results in enhanced H-bonding [44]. Therefore, their T_g increases. Furthermore, sulfonated PAES are known to exhibit multiple T_g transition temperatures [18,45]. This study observed that the presence of non-ionic and ionic-rich polymer phases resulted in lowered T_g (~235–247 °C) and upper T_g transition temperatures (~360 °C; except PAES-NMP), respectively. However, only single T_g values were observed for PAES-DMF (~360 °C). This is likely due to better solvent-polymer interaction and uniform solvent-polymer distribution. Also, the low

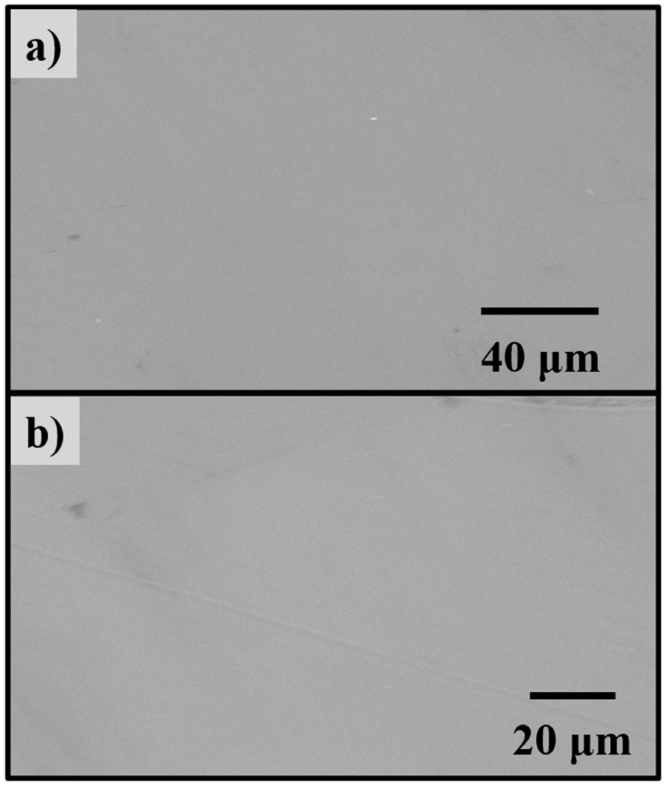

Fig. 6. SEM image showing of PAES-DMSO membrane showing smooth and crack-free microstructure (a) low magnification (b) high magnification.

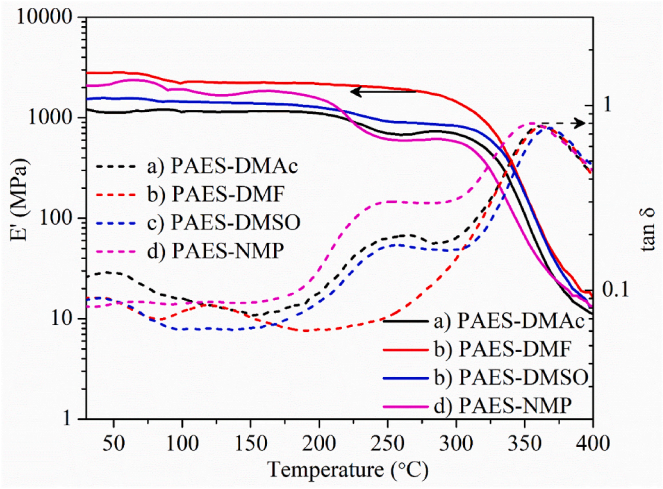

Fig. 7. Temperature ramp DMA curves showing complex modulus (solid line) and tan δ (dashed line) where (a) PAES-DMAc, (b) PAES-DMF, (c) PAES-DMSO, and (d) PAES-NMP.

molar volume of DMF results in better evaporation and the formation of a homogeneous smooth membrane surface. On the other hand, a larger molar volume of NMP and reduced interaction between PAES and NMP lowers its T_g values to ~354 °C. In this study, it was observed that among all PAES polymers, PAES-DMF exhibited the highest E' value of 1837 MPa at 303 °C while PAES-NMP exhibited the lowest E' value of ~599 MPa at 316 °C. These results reveal that the intermolecular barrier to transit the molecule is associated with the degree of stiffness of the polymer chain. Therefore, the more rigid polymer chains result in a higher T_g.

Proton conductivity of all PAES-solvent derived membranes in acid form were carried out at room temperature to achieve performance comparable to commercial standards. It was found that the proton conductivity of PAES-DMF to be 0.133 ± 0.01 S•cm^{-1} which is highest among all other PAES membranes while the PAES-DMSO membrane exhibited the lowest value of 0.103 ± 0.02 S•cm^{-1}. On the other hand, the proton conductivity of PAES-NMP and PAES-DMAc membranes were found to be similar (≈0.111 ± 0.02 S•cm^{-1}). The proton conductivity (H^+ or H_3O^+ charge carrier) of PAES membranes are due to the presence of sulfonic acid group. However, the interaction of residual solvent form hydrogen bonding with membrane could affect the proton conductivities. For instance, the residual solvents can exist either in amide II and amide III forms. NMR analysis of *N*-methyacetamide confirmed that the amide group can co-exist in different structural forms wherein 3% of amide exits in amide III structure while 0.5% can exits in amide II form [40]. Therefore, except DMSO, all solvent have the potential to exist in three foms (amide I, amide II and amide III). Since, the $\chi_{P\text{-}S}$ values of PAES-DMF (0.34) membrane are lower compared to that of PAES-NMP (0.55) and PAES-DMAc (0.57) membranes, lesser amount of residual solvent are present in PAES-DMF membrane. Therefore, the H-bonding characteristics are reduced in PAES-DMF membranes (Fig. 2). Previous studies have reported that the H-bonding interactions between the polymer and residual solvents could reduce the charge carrier number and also its proton mobility (proton conductivity) [20]. From the above discussion, it is evident that the reason for decreased proton conductivity is due to the increased H-bonding interaction of residual solvents in PAES-DMAc and PAES-NMP polymer membranes. On the other hand, PAES-DMSO exhibited the lowest proton conductivity which could probably be due to the formation of intrinsic discontinuous hydrophilic domains clusters. A separate studies are being carried out in our laboratory to understand the effect of nanodomain clusters and its influence on the proton conductivity of PAES membrane which will explain the anamolous behavior of PAES-DMSO membrane.

4. Conclusion

In this study, we report a detailed analysis of the effect of solvent on the physical, thermal and mechanical properties of PAES membranes for applications in polymer fuel cells. A correlation between residual solvent (DMF, DMSO, NMP, and DMAc), bonding characteristics, and storage modulus of the fabricated PAES membranes (PAES-DMAc, PAES-NMP, PAES-DMSO, and PAES-DMF) was established. Hensen solubility parameter (HSP) and Flory-Huggins interaction parameters confirmed that PAES polymers have a close solubility with DMF compared to other solvents and hence exhibited a better polymer-solvent interaction. DMA analysis performed on the PAES membrane derived from different solvents confirmed the presence of multiple T_g transition temperatures (except PAES-DMF) and gave an essential insight that the residual solvent in the PAES membrane acts as a plasticizer and lowers its storage modulus (E'). These findings are in line with HSP and Flory-Huggins interaction solubility parameters ($\chi_{P\text{-}S}$). This study also confirmed that the residual solvent impacts the onset of thermal degradation and correlates to HSP and $\chi_{P\text{-}S}$ parameters. Proton conductivity of PAES-DMF was found to be highest (0.133 ± 0.01 S•cm^{-1}) and were corroborated very well with the $\chi_{P\text{-}S}$ interaction parameter. This outcome will help to fabricate high-performance PAES targeted membranes with desired properties for polymer fuel cell applications.

CRediT authorship contribution statement

Natalie Y. Arnett: Project administration, Writing – review & editing, Conceptualization, Methodology, Funding acquisition, Formal analysis. **Sanjay Kumar Devendhar Singh:** Writing – original draft, Data curation, Conceptualization, Methodology. **D'Andra Moxey:** Visualization, Investigation, Methodology. **Samaiyah K.A. Mason:** Visualization, Investigation, Methodology. **Rebekah Sweat:** Writing – review & editing, Investigation, Resources. **Emily Plunket:** Writing – review & editing, Investigation, Resources. **Robert Moore:** Writing – review & editing, Investigation, Resources.

Declaration of competing interest

The authors declare that they have no known competing financial interests or personal relationships that could have appeared to influence the work reported in this paper.

Data availability

Data will be made available on request.

Acknowledgments

The authors of this paper would like to gratefully acknowledge the National Science Foundation Career Award (DMR-1454451), Arnett Polymer Research Lab, Chemistry Department, Florida A&M University, Dr. Sweat and Dr. Ramakrishnan, FAMU-FSU College of Engineering and the High-Performance Materials Institute.

Appendix A. Supplementary data

Supplementary data to this article can be found online at https://doi.org/10.1016/j.polymer.2022.125626.

References

[1] N. Calderon, E.A. Ofstead, W.A. Judy, Ring-opening polymerization of unsaturated alicyclic compounds, J. Polym. Sci. Polym. Chem. 5 (9) (1967) 2209–2217.
[2] A. Kreuchunas, Polysulfone Condensation Polymers and the Preparation of Same, Patent: US2822351A United States, 1958.
[3] P.M. Hergenrother, B.J. Jensen, S.J. Havens, Poly(arylene ethers), Polymer 29 (2) (1988) 358–369.

[4] F. Wang, M. Hickner, Y.S. Kim, T.A. Zawodzinski, J.E. McGrath, Direct polymerization of sulfonated poly(arylene ether sulfone) random (statistical) copolymers: candidates for new proton exchange membranes, J. Membr. Sci. 197 (1) (2002) 231–242.

[5] G. Maier, J. Meier-Haack, Sulfonated aromatic polymers for fuel cell membranes, in: G.G. Scherer (Ed.), Fuel Cells II, Springer Berlin Heidelberg, Berlin, Heidelberg, 2008, pp. 1–62.

[6] P. Khomein, W. Ketelaars, T. Lap, G. Liu, Sulfonated aromatic polymer as a future proton exchange membrane: a review of sulfonation and crosslinking methods, Renew. Sustain. Energy Rev. 137 (2021), 110471.

[7] N. Esmaeili, E.M. Gray, C.J. Webb, Non-fluorinated polymer composite proton exchange membranes for fuel cell applications – a review, ChemPhysChem 20 (16) (2019) 2016–2053.

[8] N.A.M. Harun, N. Shaari, N.F.H. Nik Zaiman, A review of alternative polymer electrolyte membrane for fuel cell application based on sulfonated poly(ether ether ketone), Int. J. Energy Res. 45 (14) (2021) 19671–19708.

[9] L. Assumma, H.-D. Nguyen, C. Iojoiu, S. Lyonnard, R. Mercier, E. Espuche, Effects of block length and membrane processing conditions on the morphology and properties of perfluorosulfonated poly(arylene ether sulfone) multiblock copolymer membranes for PEMFC, ACS Appl. Mater. Interfaces 7 (25) (2015) 13808–13820.

[10] H. Lee, J. Han, S.M. Ahn, H.Y. Jeong, J. Kim, H. Kim, T.-H. Kim, K. Kim, J.-C. Lee, Simple and effective cross-linking technology for the preparation of cross-linked membranes composed of highly sulfonated poly(ether ether ketone) and poly (arylene ether sulfone) for fuel cell applications, ACS Appl. Energy Mater. 3 (11) (2020) 10495–10505.

[11] L. Zhang, W. Fang, J. Jiang, Effects of residual solvent on membrane structure and gas permeation in a polymer of intrinsic microporosity: insight from atomistic simulation, J. Phys. Chem. C 115 (22) (2011) 11233–11239.

[12] N. Shiva Prasad, R. Babarao, S. Madapusi, S. Sridhar, N.R. Choudhury, S. K. Bhargava, Residual solvent induced physical morphology and gas permeation in polyamide-imide membrane: experimental investigation and molecular simulations, Eur. Polym. J. 165 (2022), 111012.

[13] A.F.M. Barton, CRC Handbook of Solubility Parameters and Other Cohesion Parameters, second ed., Taylor & Francis, 1991.

[14] G.P. Robertson, S.D. Mikhailenko, K. Wang, P. Xing, M.D. Guiver, S. Kaliaguine, Casting solvent interactions with sulfonated poly(ether ether ketone) during proton exchange membrane fabrication, J. Membr. Sci. 219 (1) (2003) 113–121.

[15] S. Dohrn, C. Luebbert, K. Lehmkemper, S.O. Kyerematen, M. Degenhardt, G. Sadowski, Solvent influence on the phase behavior and glass transition of Amorphous Solid Dispersions, Eur. J. Pharm. Biopharm. 158 (2021) 132–142.

[16] K.-S. Chang, C.-C. Hsiung, C.-C. Lin, K.-L. Tung, Residual solvent effects on free volume and performance of fluorinated polyimide membranes: a molecular simulation study, J. Phys. Chem. B 113 (30) (2009) 10159–10169.

[17] C. Van Goethem, M.M. Mulunda, R. Verbeke, T. Koschine, M. Wübbenhorst, Z. Zhang, E. Nies, M. Dickmann, W. Egger, I.F.J. Vankelecom, G. Koeckelberghs, Increasing membrane permeability by increasing the polymer crystallinity: the unique case of polythiophenes, Macromolecules 51 (23) (2018) 9943–9950.

[18] H.J. Oh, B.D. Freeman, J.E. McGrath, C.H. Lee, D.R. Paul, Thermal analysis of disulfonated poly(arylene ether sulfone) plasticized with poly(ethylene glycol) for membrane formation, Polymer 55 (1) (2014) 235–247.

[19] Y.-J. Fu, C.-C. Hu, H.-z. Qui, K.-R. Lee, J.-Y. Lai, Effects of residual solvent on gas separation properties of polyimide membranes, Separ. Purif. Technol. 62 (1) (2008) 175–182.

[20] R. Guan, H. Dai, C. Li, J. Liu, J. Xu, Effect of casting solvent on the morphology and performance of sulfonated polyethersulfone membranes, J. Membr. Sci. 277 (1) (2006) 148–156.

[21] M. Lee, J.K. Park, H.-S. Lee, O. Lane, R.B. Moore, J.E. McGrath, D.G. Baird, Effects of block length and solution-casting conditions on the final morphology and properties of disulfonated poly(arylene ether sulfone) multiblock copolymer films for proton exchange membranes, Polymer 50 (25) (2009) 6129–6138.

[22] R.S. Okor, W. Anderson, Casting solvent effects on the permeability of polymer films of differing quaternary ammonium (cation) content, J. Pharm. Pharmacol. 39 (7) (2011) 547–548.

[23] J. Kim, B. Kim, B. Jung, Y.S. Kang, H.Y. Ha, I.-H. Oh, K.J. Ihn, Effect of casting solvent on morphology and physical properties of partially sulfonated polystyrene-block-poly(ethylene-ran-butylene)-block-polystyrene copolymers, Macromol. Rapid Commun. 23 (13) (2002) 753–756.

[24] A. Carbone, R. Pedicini, G. Portale, A. Longo, L. D'Ilario, E. Passalacqua, Sulphonated poly(ether ether ketone) membranes for fuel cell application: thermal and structural characterisation, J. Power Sources 163 (1) (2006) 18–26.

[25] J. Xi, Z. Li, L. Yu, B. Yin, L. Wang, L. Liu, X. Qiu, L. Chen, Effect of degree of sulfonation and casting solvent on sulfonated poly(ether ether ketone) membrane for vanadium redox flow battery, J. Power Sources 285 (2015) 195–204.

[26] T.N. Thompson, N.Y. Arnett, Effect of phosphonated triazine monomer additive in disulfonated poly (arylene ether sulfone) composite membranes for proton exchange membrane fuel cells, Polymer 171 (2019) 34–44.

[27] N.Y. Arnett, Synthesis and Characterization of Disulfonated Poly(arylene Ether Sulfone) Random Copolymers as Multipurpose Membranes for Reverse Osmosis and Fuel Cell Applications, Macromolecular Science and Engineering Virginia Polytechnic Institute and State University, 2009.

[28] R.J. Cotter, Engineering plastics, in: A Handbook of Polyarylethers, Taylor & Francis, 1995.

[29] D.W. van Krevelen, Properties of Polymers, Elsevier Science, 2012.

[30] C.M. Hansen, The Three Dimensional Solubility Parameter - Key to Paint Component Affinities: I. Solvents, Plasticizers, Polymers, and Resins, 1967.

[31] C.L. Aitken, J.S. McHattie, D.R. Paul, Dynamic mechanical behavior of polysulfones, Macromolecules 25 (11) (1992) 2910–2922.

[32] S. Liu, Y. Jing, J. Tu, H. Zou, Z. Yong, G. Liu, Systematic investigation on the swelling behaviors of acrylonitrile-butadiene rubber via solubility parameter and Flory-Huggins interaction parameter, J. Appl. Polym. Sci. 139 (20) (2022), 52172.

[33] N.D. Sankir, R.O. Claus, J.B. Mecham, W.L. Harrison, Electrically conductive polyaniline-sulfonated poly(arylene ether sulfone) composites, Appl. Phys. Lett. 87 (24) (2005), 241910.

[34] H. Hou, F. Vacandio, M.L.D. Vona, P. Knauth, Sulfonated polyphenyl ether by electropolymerization, Electrochim. Acta 81 (2012) 58–63.

[35] D. Bakarić, J. Alerić, T. Parlić-Risović, J. Spanget-Larsen, Hydrogen bonding between ethynyl aromates and triethylamine: IR spectroscopic and computational study, Spectrochim. Acta: Mol. Biomol. Spectrosc. 209 (2019) 288–294.

[36] X. Liu, S. He, S. Liu, H. Jia, L. Chen, B. Zhang, L. Zhang, J. Lin, The roles of solvent type and amount of residual solvent on determining the structure and performance of sulfonated poly(ether ether ketone) proton exchange membranes, J. Membr. Sci. 523 (2017) 163–172.

[37] B. Athokpam, S.G. Ramesh, R.H. McKenzie, Effect of hydrogen bonding on the infrared absorption intensity of OH stretch vibrations, Chem. Phys. 488–489 (2017) 43–54.

[38] T. Fornaro, D. Burini, M. Biczysko, V. Barone, Hydrogen-bonding effects on infrared spectra from anharmonic computations: uracil–water complexes and uracil dimers, J. Phys. Chem. A 119 (18) (2015) 4224–4236.

[39] G. Mridula, N. Ananth N, M.G. Netkal M, Theoretical study of hydrogen bonded picolinic acid-water complexes, Indian J. Chem. 55 (2016) 782–792.

[40] Y. Ji, X. Yang, Z. Ji, L. Zhu, N. Ma, D. Chen, X. Jia, J. Tang, Y. Cao, DFT-calculated IR spectrum amide I, II, and III band contributions of N-methylacetamide fine components, ACS Omega 5 (15) (2020) 8572–8578.

[41] S. Kaliaguine, S.D. Mikhailenko, K.P. Wang, P. Xing, G. Robertson, M. Guiver, Properties of SPEEK based PEMs for fuel cell application, Catal. Today 82 (1) (2003) 213–222.

[42] S. Samitsu, Fabrication of mesoporous crystalline microparticles of poly(ether sulfone) via solvent-induced crystallization, Polymer 248 (2022), 124744.

[43] E. Sgreccia, J.F. Chailan, M. Khadhraoui, M.L. Di Vona, P. Knauth, Mechanical properties of proton-conducting sulfonated aromatic polymer membranes: stress–strain tests and dynamical analysis, J. Power Sources 195 (23) (2010) 7770–7775.

[44] G. Li, C. Zhao, X. Li, D. Qi, C. Liu, F. Bu, H. Na, Novel side-chain-type sulfonated diphenyl-based poly(arylene ether sulfone)s with a hydrogen-bonded network as proton exchange membranes, Polym. Chem. 6 (32) (2015) 5911–5920.

[45] Y. Kwon, S.Y. Lee, S. Hong, J.H. Jang, D. Henkensmeier, S.J. Yoo, H.-J. Kim, S.-H. Kim, Novel sulfonated poly(arylene ether sulfone) containing hydroxyl groups for enhanced proton exchange membrane properties, Polym. Chem. 6 (2) (2015) 233–239.